Using ExoMars-TGO/CaSSIS for the spatial and spectral characterization of hematite-rich locations on Mars

Éloïse Brassard[1], Livio L. Tornabene[2,3], Myriam Lemelin[1] and Ed Cloutis[4]

[1]Dept. Géomatique Appliquée, Univ. de Sherbrooke, Canada; [2]Dept. Earth Sciences, Univ. Western Ontario, Canada; [3]Inst. Space & Earth Exploration, Univ. Western Ontario, Canada; [4]Dept. Geography, Univ. of Winnipeg, Canada.

Corresponding author: eloise.brassard@usherbrooke.ca

EPSC abstract #285

1. INTRODUCTION AND OBJECTIVE

Hematite has been detected on Mars using orbital and rover instruments (Fig. 1):

- Global orbital studies using low spatial resolution datasets (e.g., MGS/TES, MEX/OMEGA, both ~3–10 km/px)
  - → Large regions as Meridiani Planum, Aram and Aureum Chaos [1,2,3]
- Local orbital studies using high spectral and spatial resolution datasets (e.g., oversampled MRO/CRISM, 6–8 m/px)
  - → Small regions as Vera Rubin Ridge in Gale Crater [4]
- Rover ground analysis: Opportunity and Curiosity identified hematite [5,6]

Hematite presence is suggested as evidence of ancient aqueous settings [1,2,4,7]:

- Most of its formation mechanisms involve water [8,9] and may involve microbial activity, which could be preserved [8]
- Hematite occurrences may thus hint at past potential habitable environments

Our objective is to refine global-scale mapping of hematite occurrences on Mars using a combination of high spatial and spectral resolution orbital images acquired by the TGO/CaSSIS, MRO/CRISM and MRO/HiRISE instruments.

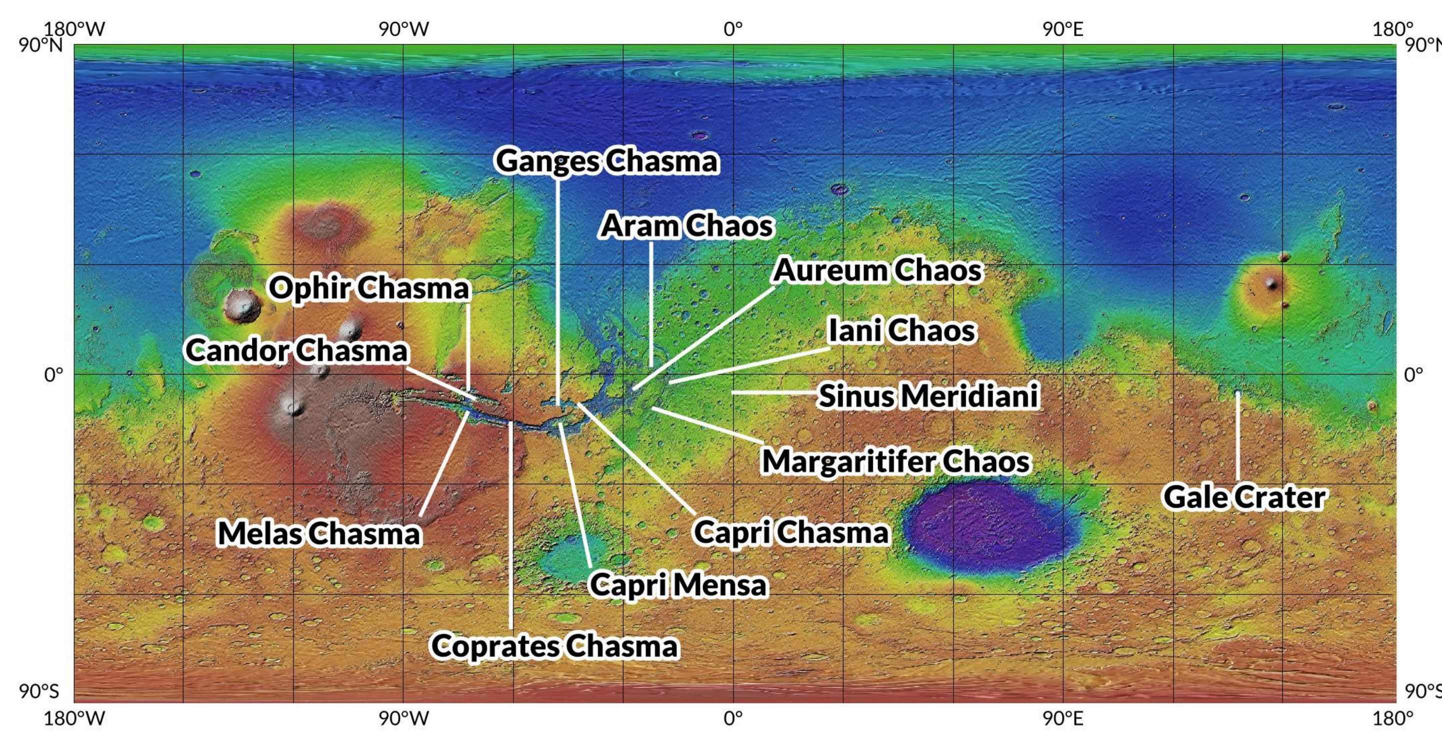

Fig. 1. Regions on Mars where hematite-rich locations have been identified in previous studies. Basemap: MOLA topography and THEMIS IR blend.

2. DATASETS

ExoMars Trace Gas Orbiter (2016, ESA)

Colour and Stereo Surface Imaging System (CaSSIS) [10]

- 4 VNIR bands at ~4 m/px
- BLU: 495 nm — PAN: 678 nm — RED: 836 nm — NIR: 939 nm

Allows for near-unique identification of hematite in NRP colour composite images (magenta colour) [11] (Fig. 2)

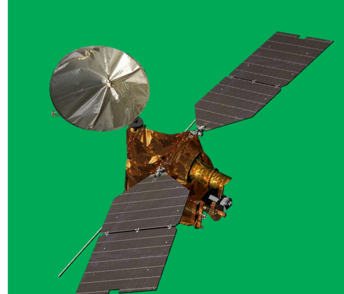

Mars Reconnaissance Orbiter (2005, NASA) [12]

Compact Reconnaissance Imaging Spectrometer for Mars (CRISM)

- 107 VNIR + 438 IR hyperspectral bands at 18–36 m/px
- VNIR Hyperspectral Data Records (VRDR) at 90 m/px, 90 bands

BD530, BD920 and BDI1000VIS spectral indices are used to locate regions that may contain crystalline hematite in the VRDRs [13]

High Resolution Imaging Experiment (HiRISE)

- 3 VNIR bands at 25–50 cm/px
- BG: <580 nm — RED: 570–830 nm — NIR: >790 nm

Allows for detailed morphologic and textural observations

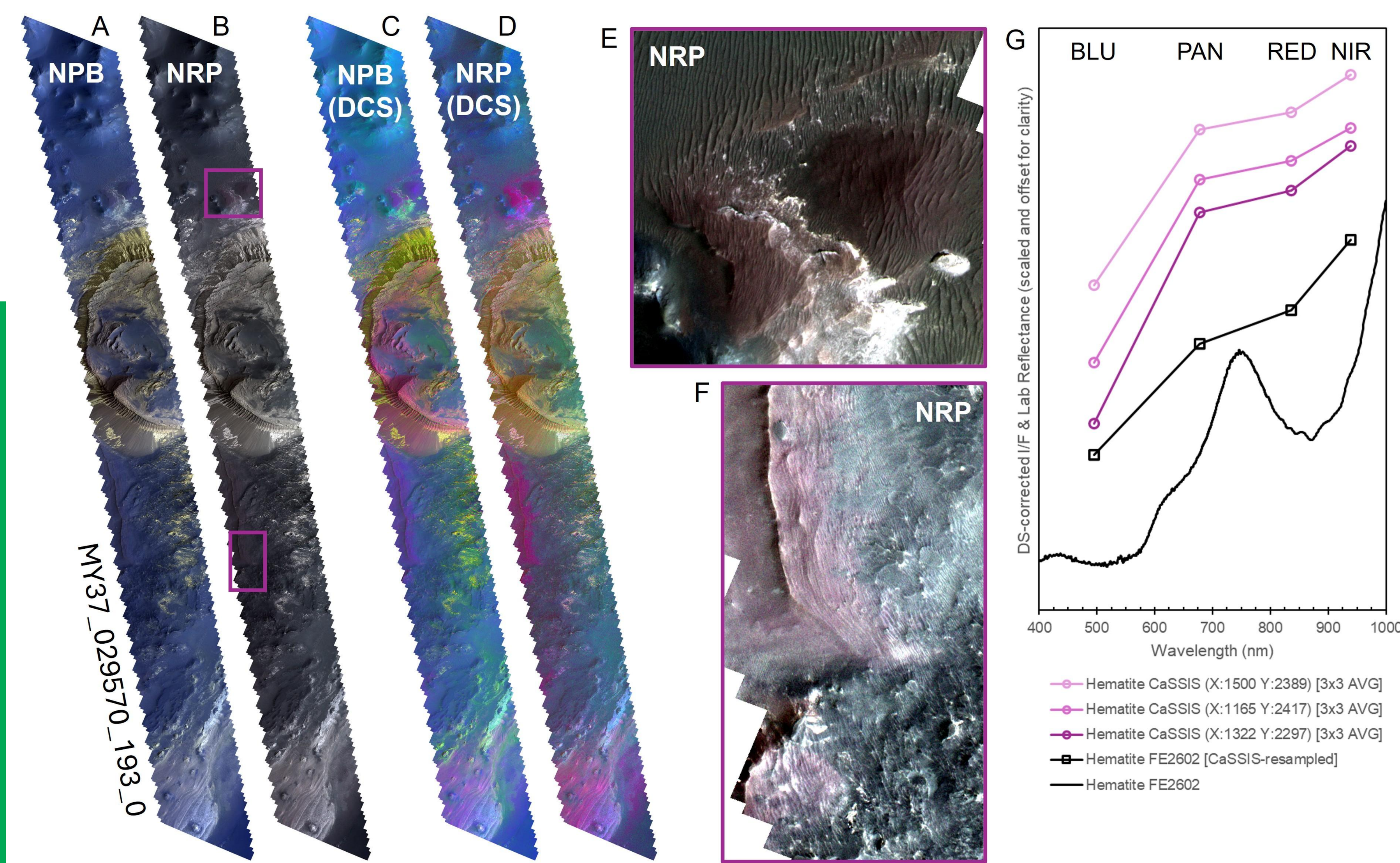

Fig. 2. Dark Subtraction corrected CaSSIS image MY37_029570_193_0 in Capri Chasma. (A and B) NPB and NRP colour composite (0.1% linear stretch). Purple rectangles indicate the location of insets E and F. (C and D) Decorrelation colour stretched (DCS) image based on A and B (0.1% linear stretch). NRP DCS (D) highlights in pink the hematite-rich regions, whereas NPB DCS (C) provides weaker contrast for these regions. (E and F) Hematite-rich locations exhibiting a dark magenta colour in NRP relative to the greyish background (linear stretch of 2% and 1% respectively). (G) CaSSIS-extracted spectra (purple circles), compared to hematite lab reference spectrum (USGS: FE2602) resampled to CaSSIS wavelengths (black squares).

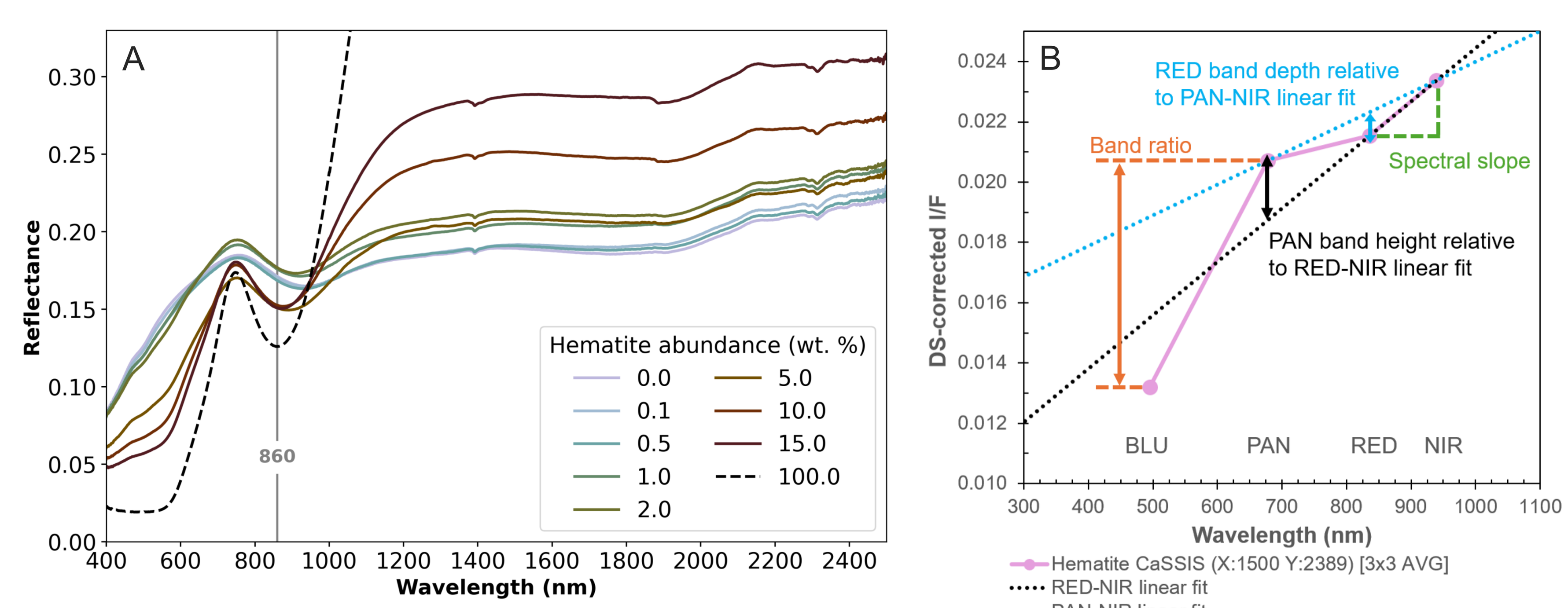

Fig. 3. (A) Reflectance of mixtures of fine-grained red hematite and planetary simulant (LMS-1) representing the abundance range observed on Mars. The 860 nm absorption feature is marked. (B) Spectral parameters used to distinguish hematite from other Mars minerals (band ratio, spectral slope, band depth, and band height). Examples of a "classical" band depth, measured relative to a linear fit between bands bracketing the feature (dotted blue), and a "modified" band height, measured relative to a linear fit using any band combination (dotted black), are shown.

3. METHODS

3.1. Laboratory sample characterization (VNIR spectroscopy)

- Estimate the detection limit of fine-grained hematite by hyperspectral ground sensors and simulated multispectral orbital sensors via the analysis of mixtures of fine-grained red hematite and planetary simulant [14] (Fig. 3A)

3.2. Survey of known hematite occurrences

- Review of literature and existing datasets to identify known occurrences (Fig. 1)

3.3. CaSSIS spectral parameters assessment

- Comprehensive suite of CaSSIS spectral parameters calculated on a spectral library of Martian minerals [15] (Fig. 3B)
- Statistical methods used to assess which parameter combinations are the most useful to distinguish between hematite and other minerals, and to investigate the distinction of other iron minerals (goethite, jarosite, ferrihydrite) [15]

3.4. CaSSIS–CRISM–HiRISE combined analysis

- Spectral parameters applied to the CaSSIS data to produce a refined global-scale mapping of hematite, and potentially other ferric iron minerals, at unprecedented spatial resolution. This mapping effort is expected to reveal previously undetected small hematite-rich occurrences.
- High-spatial-resolution spectral analysis and characterisation of hematite occurrences using CaSSIS, CRISM and HiRISE images/products corrected using a Dark Subtraction (DS) method to account for atmospheric scatter [16,17]

4. RESULTS AND FUTURE WORK

- Laboratory sample characterisation indicates a hematite detection limit of ≥ 2 wt. % for VNIR hyperspectral ground data and a limit of ≥ 5 wt. % for VNIR multispectral orbital data [14]
- From the literature, 83 hematite occurrences were identified within 14 regions
- The CaSSIS spectral parameters assessment and the CaSSIS–CRISM–HiRISE combined analysis are currently underway

GEODES laboratory (GEOmatics Dedicated to the Exploration of Space)

Fonds d'appui à l'engagement étudiant (FAEE) de l'Université de Sherbrooke

Bourses d'études supérieures du Canada Vanier / Canada Graduate Scholarships

CANADA RESEARCH CHAIRS / CHAIRES DE RECHERCHE DU CANADA

References

[1] Christensen et al. (2001) *JGR: Planets*, 106(E10). [2] Glotch and Rogers (2007) *JGR: Planets*, 112(E6), E06001. [3] Carrozzo et al. (2012) *JGR: Planets*, 117(E11), E00J17. [4] Fraeman et al. (2013) *Geology*, 41(10). [5] Squyres et al. (2004) *Science*, 306(5702). [6] Rampe et al. (2020) *Geochemistry*, 80(2), 125605. [7] Yoshida et al. (2018) *Sci. Adv.*, 4(12). [8] Allen et al. (2001) *Astrobiology*, 1(1). [9] Jiang et al. (2022) *Rev. Geophys.*, 60(1), e2020RG000698. [10] Thomas et al. (2017) *Space Sci. Rev.*, 212. [11] Tornabene et al. (2024) EPSC abstract 1321. [12] Zurek and Smrekar (2007) *JGR: Planets*, 112(E5). [13] Murchie et al. (2025) EPSC abstract 136. [14] Brassard et al. (2025) LPSC abstract 2420. [15] Stabbins et al. (2024) *Earth Space Sci.*, 11(10), e2023EA003398. [16] Tornabene et al. (2018) *Space Sci. Rev.*, 214(18). [17] Rangarajan et al. (2024) *Icarus*, 419, 115849.